International Research Journal of Engineering and Technology (IRJET) e-ISSN: 2395-0056
Volume: 10 Issue: 07 | July 2023 www.irjet.net p-ISSN: 2395-0072

# Fail Safe Design of Skin and Bulkhead of an Aircraft Stiffened Panel by Residual Strength Evaluation Method

**Shivanandappa N D[1], Srinivasa Murthy M K[2], Guru Kiran E[3]**

*[1]Assistant Professor, Dept. of Mechanical Engineering, J N N College of Engineering, Shivamogga, Karnataka, India.*
*[2]Assistant Professor, Dept. of Mechanical Engineering, J N N College of Engineering, Shivamogga, Karnataka, India.*
*[3]PG Student, Dept. of Mechanical Engineering, J N N College of Engineering, Shivamogga, Karnataka, India.*

---

***Abstract -*** *The failsafe design of aircraft structural components is a critical aspect of modern aviation engineering, ensuring the safety and reliability of aircraft in the face of potential failures. With the ever-increasing demands for air travel and the continuous push towards technological advancements, the design of aircraft structural components must adhere to rigorous standards to withstand unforeseen challenges. Stiffened panel is one such component part which is prone to crack initiation and houses many smaller components. All these subcomponents must withstand the applied load in the presence of crack and fluctuating loads for the safety of stiffened panel. Residual strength determination is performed for evaluating the design of the skin and bulkheads. The method involves the finite element analysis of the panel with crack to determine the stress intensity factor by modified virtual crack closure integral method and the maximum stress developed in the components. The residual strength of skin and bulkhead for three different skin thicknesses and varying crack lengths are determined and analysed to estimate the safety of the panel. The results show that the skin offers more resistance to crack propagation as the thickness increases. Also, the result shows that the residual strength of the components increases as the thickness of skin is increased.*

**Keywords** —Fail-safe Design, Fracture Toughness, MVCCI method, Stiffened Panel, Residual Strength.

## 1 INTRODUCTION

The damage tolerance and airworthiness requirements must be met for the aircraft to fly safely. A structure is said to be damage tolerant if it continues to function even after an initial damage is discovered. The analysis of fatigue crack propagation is the primary focus while evaluating the damage tolerance. It entails figuring out how fractures spread throughout the service life.

Modern aircraft operate in a complicated environment with varying loading circumstances, resource constraints, and economic demands. The primary aeroplane parts are built to meet specific static and dynamic loading conditions, deformation requirements, and functioning requirements. Service loads during an aircraft's operation are crucial for both design and durability and damage tolerance testing. A significant difficulty in aircraft design is fatigue and the ensuing fracture growth. Fatigue and damage tolerance design, analysis, testing, and service experience correlation are crucial for maintaining an aircraft's airworthiness during its entire economic service life.

A plane's design takes into account determining the ideal ratios between payload and vehicle weight. It must be rigid and powerful enough to fly in unusual situations. Additionally, the aircraft must fly even if a component malfunctions while it is in flight.

In contemporary aircraft, the skin serves as a load-bearing element. Unlike flat sheets, which can only support tension, folded sheet metals may support compressive stresses. Stiffeners, when paired with a piece of skin, are analysed as stringers, which are thin-walled structures.

In the present scenario, a portion of the fuselage segment's stiffened panel is taken into consideration for the analysis and then put through tensile loading that is equal to the hoop stress created in the fuselage. Fuselage damage must not go beyond the design limit and must not cause the structure to fail catastrophically, which would destroy the aircraft's structural integrity. Therefore, damage tolerance should be included in the design of the structure to prevent structural failure. By thickening the skin of the stiffened panel, the damage to the skin in this situation can be endured.

The geometric model of the stiffened panel with fuselage segment has been created in CATIA modeling software and then imported into MSC.PATRAN for finite element modeling. The finite element model is solved using MSC.NASTRAN for solving stiffened panel subjected to the tensile loading with a center crack.

## 2 LITERATURE SURVEY

T. Swift[1] proposed new concepts on fatigue and damage tolerance capability of pressurized fuselage structure is extremely sensitive to stress level, geometrical design, and material choice. They have attempted to describe the development of fracture technology related to the design of pressurized fuselage structure capable of sustaining large, easily detectable damage.

Toor[2] has worked extensively on damage tolerant design approaches applied to aircraft structures. It was concluded that simple methods of fracture mechanics can be utilized for finding the degree of damage tolerance.

J.F.M. Wiggenraad and P.Arendsen[3] have investigated the importance of die design to be damage tolerant during different stages of damage.

N.K. Salgado, M.H. Aliabadi[4] investigated crack growth analysis in stiffened panels by finite element analysis technique. The stress intensity factors were found out from the analysis.

For load bearing capability and fracture growth traits under distributed tensile load, M. Adeel[5] has assessed conventional and integrated stiffened panels. The crack growth characteristics foundout from finite element analysis for each type of panels are compared.

ShamsuzuhaHabeeb, K.S.Raju[6] have analysed a four stringer stiffened panel with a central crack for crack arrest and load bearing capabilities. It is found that the strength of the stiffened panel has reduced when compared to unstiffened panel.

F.Carta, A.Pirondi[7] have studied on the effect of bonded reinforcements between skin and stiffener to determine the crack propagation rate in the skin. The results obtained from finite element analysis are in close proximity to experimental results.

## 3 MATERIALS AND METHODOLOGY:

The following steps are adopted in evaluating the stress intensity factor of a cracked stiffened panel.

1. Development of a geometric model of the stiffened panel with all of its component parts.
2. Estimation of loads on the stiffened panel.
3. Analysis of stiffened panel using finite element method.
4. Evaluation of the stress intensity factor using the MVCCI method for different stiffened panel thicknesses.

### 3.1 GEOMETRIC CONFIGURATION OF THE STIFFENED PANEL

As the principal component of the fuselage to which all elements are connected, the stiffened panel as depicted in figure 3.1 must be able to withstand bending moments, torsional loads, and cabin pressurization.

**Figure 3.1:** Fuselage of an aircraft

A segment of the stiffened panel considered for the finite element analysis is as shown in figure 3.2

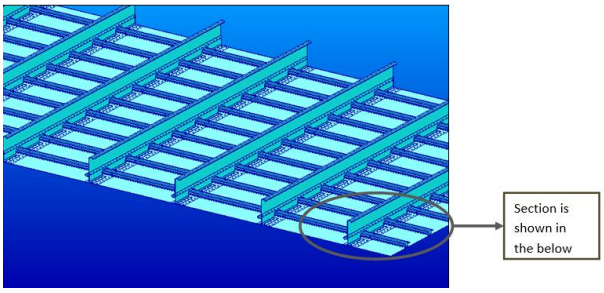


**Figure 3.2:** Geometric model of stiffened panel

Figure 3.3 shows the stiffened panel's component parts.

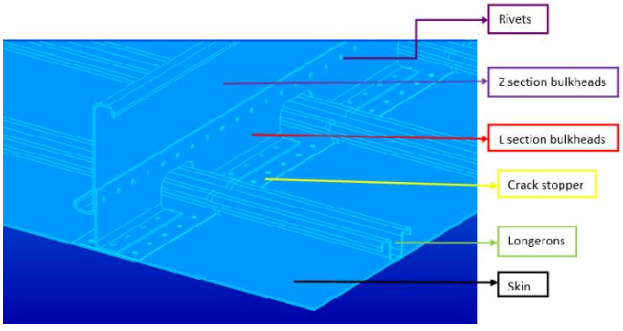


**Figure 3.3:** Enlarge view of stiffened panel

In table 3.1, the sizes and materials of each component are listed. All measurements are given in millimeters.

**Table 3.1:** Dimensions of stiffened panel components

| Name of the Parts | Dimensions in mm | Thickness in mm | Material | Number |
|---|---|---|---|---|
| Bottom Skin | 1905×3556 | 1.8 | Al | 1 |
| Bulkhead L stringer- Bottom Flange Web Flange | 1905×23.6 1905×56.0 | 1.8 1.8 | Al | 7 |
| Bulkhead Z Frames Top Flange Bottom Flange Web | 1905×9.525 1905×24.02 1905×114.3 | 1.8 1.8 1.8 | Al | 7 |
| Longerons Side Flange Top Flange Web Bottom Flange Web Top Flange Side Flange | 3556×8.381 3556×16.09 3556×25.40 3556×22.22 3556×25.4 3556×16.09 3556×8.381 | 1.8 1.8 1.8 1.8 1.8 1.8 1.8 | Al | 9 |
| Crack stopper | 1905×76.12 | 1.8 | Al | 7 |
| Rivets | Diameter | 4.4 | Al | 4830 |

The general part of the fuselage section is made up of stiffened panels. The fuselage is made up of several strengthened panels integrated together. The geometric model used for the analysis is the same as the actual fuselage stiffening panel. The meshing is done with the assumption that the curved panel is a straight panel for analysis purposes. The stiffened panel's numerous components are arranged geometrically as indicated in figures 3.4 to 3.9.

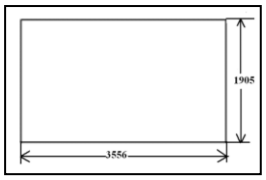


**Figure 3.4:** Dimensions of skin

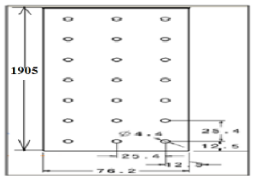


**Figure 3.5:** Dimensions of crack stopper

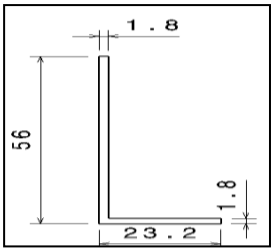


**Figure 3.6:** Dimensions of L bulkhead

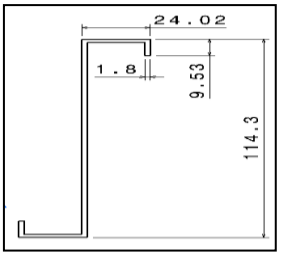


**Figure 3.7:** Dimensions of Z bulkhead

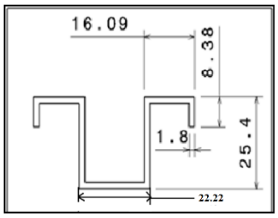


**Figure 3.8:** Dimensions of Longerons

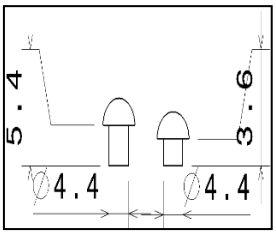


**Figure 3.9:** Dimensions of rivets

## 3.2 ESTIMATION OF LOADS IN THE STIFFENED PANEL:

The fuselage of an aircraft structure is subjected to an internal pressurization in the range of 0-10 psi. Aircraft structure is generally cylindrical in nature and is subjected to hoop stress. As the stiffened is modeled as straight panel the hoop stresses are converted into corresponding tensile stresses acting on the components.

Hoop stress is given by

$$\sigma_{hoop} = \frac{p_i \times r_i}{B} \quad (3.1)$$

The hoop stress is calculated by assuming the following values.
Cabin pressure, pi = 6 psi
Radius of the fuselage, ri = 1500 mm
Thickness of skin, B = 1.8 mm
$\boldsymbol{\sigma_{hoop} = 34.335\ Mpa}$

$\sigma_{hoop} = \sigma_{tensile} = \frac{F}{A}$ (3.2)

$F = \sigma_{hoop} \times A$ (3.3)

Force per unit length i.e. the load acting along the length is calculated by

$q = \frac{F}{L} = \sigma_{hoop} \times t$ (3.4)

Force per unit length acting on the skin, stopper and bulkhead are calculated by the following equations:

$q_s = \sigma_{hoop} \times t_s$ (3.5)

$\boldsymbol{q_s = 61.803\ N/mm}$

$q_c = \sigma_{hoop} \times t_c$ (3.6)

$\boldsymbol{q_c = 21.803\ N/mm}$

$q_b = \sigma_{hoop} \times t_b$ (3.7)

$\boldsymbol{q_b = 61.803\ N/mm}$

## 3.3 FINITE ELEMENT ANALYSIS OF STIFFENED PANEL

The stiffened panel's components are all made of aluminum 2024 T3 alloy. Table 3.2 provides a summary of the Aluminum 2024 T3's properties.

**Table 3.2:** Material properties of Aluminium 2024 T3

| SN | Property | Value |
|---|---|---|
| 1 | Young's modulus | 73 GPa |
| 2 | Poisson's ratio | 0.3 |
| 3 | Ultimate tensile strength | 483 MPa |
| 4 | Ultimate shear strength | 283 MPa |
| 5 | Fracture toughness | 37MPa$\sqrt{m}$ |

The finite element analysis of the stiffened panel is carried out using NASTRAN solver. Meshing is done on the components using quadrilateral and triangular shell elements. The crack is introduced at the center of the skin by disconnecting the common nodes of the elements on the crack front. The region near the crack tip is fine meshed with an edge length of 0.8 mm to avoid the stress singularity. The rest of the portion is meshed with coarse mesh.

Initially the structure is analyzed for a skin thickness of 1.8 mm and a central crack of 2a = 25.4 mm. One end of the stiffened panel which is parallel to the crack is fully constrained and the other end is subjected to loads as shown in figure 3.1

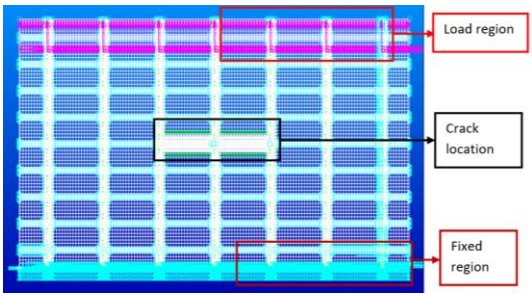


**Figure 3.10:** Meshed panel with loads and boundary conditions

Assuming that the maximum damage occurs to the panel when the bulk heads are broken i.e. as the crack passes through the bulkheads. The broken bulkheads are modeled by deleting the elements in that region. The deformation plot of the above model is shown in figure 3.11. The plot indicates that there is a deformation in Z direction. In order to avoid bending of the stiffened panel, the deformation in Z direction needs to be constrained at all the nodes and the model is analysed by introducing the new boundary conditions as shown in figure 3.12.

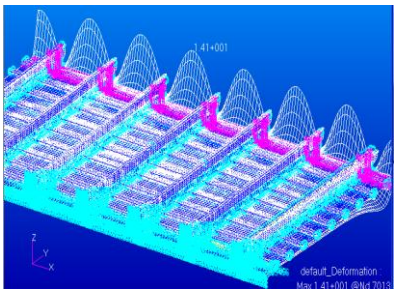

**Figure 3.11:** Deformation plot of stiffened panel without constraining in Z direction

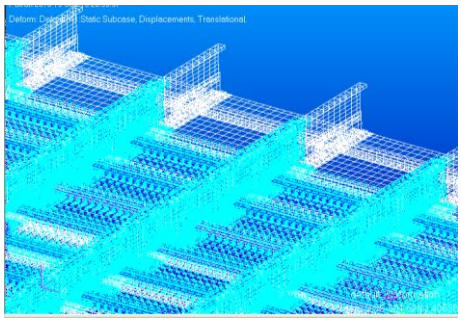

**Figure 3.12:** Deformation plot of stiffened panel with constraint in Z direction

### 3.4 SIF calculation using the MVCCI method for 1.8 mm of skin thickness

After the completion of the FE analysis, the modified virtual crack closure method is used to compute the SIF of the loaded panel, and the results are tabulated as shown in table 3.3.

**Table 3.3**: SIF values for different Skin thickness

| Crack length (2a) in mm | $K_{I(FEA)}$ in MPa$\sqrt{m}$ | | |
|---|---|---|---|
| | Skin thickness 1.8 mm | Skin thickness 2.0 mm | Skin thickness 2.2 mm |
| 25.40 | 14.48 | 12.81 | 11.47 |
| 76.20 | 23.10 | 20.53 | 18.44 |
| 127.0 | 26.44 | 23.67 | 21.42 |
| 177.8 | 28.45 | 25.64 | 23.33 |
| 228.6 | 30.96 | 28.02 | 25.60 |
| 279.4 | 32.08 | 29.13 | 26.68 |
| 330.2 | 33.77 | 30.75 | 28.22 |
| 381.0 | 35.39 | 32.29 | 29.69 |
| 431.8 | 36.93 | 33.76 | 31.10 |
| 482.6 | 38.14 | 35.17 | 32.45 |
| 533.4 | 39.81 | 36.52 | 33.73 |
| 584.2 | 41.52 | 37.79 | 34.96 |
| 635.0 | 42.37 | 38.99 | 36.12 |
| 685.8 | 43.49 | 40.08 | 37.19 |
| 736.6 | 44.46 | 41.06 | 38.15 |
| 787.4 | 45.24 | 41.86 | 38.96 |
| 838.2 | 45.73 | 42.14 | 39.56 |
| 889.0 | 45.77 | 42.57 | 39.81 |
| 939.8 | 44.98 | 42.02 | 39.43 |
| 990.6 | 41.86 | 39.41 | 37.23 |
| 1016 | 39.78 | 37.93 | 36.22 |

## 4 RESIDUAL STRENGTH OF THE STIFFENED PANEL COMPONENTS

A fracture can have a major impact on a structure's strength, which is often much lower than the strength of the undamaged structure. One must assess the load carrying capability that will exist in the potentially fractured structure during its anticipated service life to avoid catastrophic failure. The residual strength of a cracked structure, which depends on the material toughness, crack size, crack geometry, and structural design, determines how much load the structure can support. As seen in Figure 4.1, the strength decreases as damage size increases. To permit unrestricted operational utilization, it becomes important to maintain limit load capability.

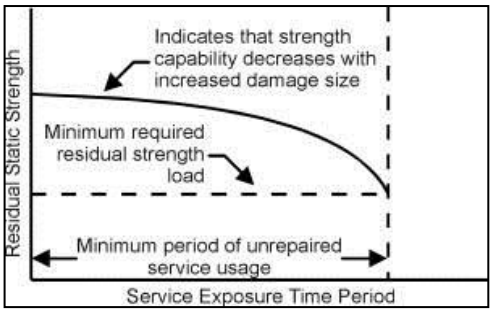


**Figure 4.1:** Residual strength diagram

### 4.1 Residual Strength for Skin

Residual strength for skin is calculated by the following equation.

$$Residual\ Strength = \frac{K_{IC}}{K_I} \times \sigma_R \quad (4.1)$$

Where $K_{IC}$ is the fracture toughness of the material of the skin. $K_I$ is the stress intensity factor of the skin. $\sigma_R$ is the remotely applied stress.

The calculation and tabulation of residual strength for a skin with three different thicknesses is shown in table 4.1.

**Table 4.1:** Residual strength of skin for various skin thickness

| Crack length (2a) in mm | Residual strength in MPa | | |
|---|---|---|---|
| | Skin thickness 1.8 mm | Skin thickness 2.0 mm | Skin thickness 2.2 mm |
| 25.40 | 87.73 | 99.17 | 110.75 |
| 76.20 | 54.92 | 61.87 | 68.89 |
| 127.0 | 48.04 | 53.68 | 59.30 |
| 177.8 | 44.56 | 49.54 | 54.45 |
| 228.6 | 41.89 | 46.29 | 50.69 |
| 279.4 | 39.60 | 43.61 | 47.61 |
| 330.2 | 37.61 | 41.31 | 45.01 |
| 381.0 | 35.89 | 39.41 | 42.78 |
| 431.8 | 34.40 | 37.63 | 40.84 |
| 482.6 | 33.30 | 36.13 | 39.14 |
| 533.4 | 31.19 | 34.78 | 37.66 |
| 584.2 | 30.59 | 33.61 | 36.33 |
| 635.0 | 29.98 | 32.58 | 35.17 |
| 685.8 | 29.21 | 31.69 | 34.15 |
| 736.6 | 28.57 | 30.93 | 33.30 |
| 787.4 | 28.08 | 30.34 | 32.85 |
| 838.2 | 27.78 | 29.95 | 32.11 |
| 889.0 | 27.32 | 29.54 | 31.90 |
| 939.8 | 28.24 | 30.23 | 32.21 |
| 990.6 | 30.34 | 32.23 | 34.12 |
| 1016 | 31.93 | 33.49 | 35.06 |

### 4.2 Residual strength for bulkhead

Residual strength for bulkhead is defined by the equation 4.2.

$$Residual\ Strength = \frac{\sigma_u}{\sigma_{Max}} \times \sigma_R \qquad (4.2)$$

Where $\sigma_u$ is the ultimate tensile strength of the material of the bulkhead. $\sigma_{Max}$ is the maximum stress developed in the bulkhead.

The maximum stress developed in the bulkhead is obtained by performing the finite element analysis and are tabulated in table 4.1.

**Table 4.2:** Maximum stress of bulkhead for various skin thickness

| Crack length (2a) in mm | Maximum stress in MPa | | |
|---|---|---|---|
| | Skin thickness 1.8 mm | Skin thickness 2.0 mm | Skin thickness 2.2 mm |
| 25.40 | 82.0 | 76.50 | 71.7 |
| 76.20 | 82.4 | 77.40 | 72.0 |
| 127.0 | 83.0 | 78.60 | 72.6 |
| 177.8 | 84.0 | 79.00 | 73.4 |
| 228.6 | 85.1 | 79.60 | 74.3 |
| 279.4 | 86.4 | 81.20 | 75.4 |
| 330.2 | 87.8 | 82.30 | 76.6 |
| 381.0 | 89.6 | 84.30 | 78.1 |
| 431.8 | 91.5 | 86.10 | 79.9 |
| 482.6 | 93.8 | 88.80 | 81.9 |
| 533.4 | 96.5 | 90.80 | 84.2 |
| 584.2 | 99.5 | 94.80 | 87.0 |
| 635.0 | 103 | 97.80 | 90.2 |
| 685.8 | 107 | 101.9 | 94.0 |
| 736.6 | 112 | 107.0 | 98.6 |
| 787.4 | 119 | 113.0 | 104 |
| 838.2 | 126 | 118.4 | 111 |
| 889.0 | 136 | 126.4 | 120 |
| 939.8 | 148 | 139.0 | 131 |
| 990.6 | 163 | 153.0 | 145 |
| 1016 | 173 | 162.0 | 156 |

The residual strength of the bulkhead for various skin thicknesses is evaluated by equation 4.2 and are tabulated in table 4.3.

**Table 4.3:** Residual strength of bulkhead for various skin thickness

| Crack length (2a) in mm | Residual strength in MPa | | |
|---|---|---|---|
| | Skin thickness 1.8 mm | Skin thickness 2.0 mm | Skin thickness 2.2 mm |
| 25.40 | 202.24 | 216.78 | 231.29 |
| 76.20 | 201.25 | 214.26 | 230.33 |
| 127.0 | 199.80 | 210.98 | 228.40 |
| 177.8 | 197.42 | 209.92 | 225.90 |
| 228.6 | 194.87 | 208.33 | 223.20 |
| 279.4 | 191.94 | 204.23 | 219.90 |
| 330.2 | 188.88 | 201.50 | 216.40 |
| 381.0 | 185.08 | 196.72 | 212.30 |
| 431.8 | 181.24 | 192.61 | 207.55 |
| 482.6 | 176.79 | 186.75 | 202.48 |
| 533.4 | 171.85 | 182.64 | 196.90 |
| 584.2 | 166.67 | 174.93 | 190.60 |
| 635.0 | 161.00 | 169.56 | 183.85 |
| 685.8 | 154.98 | 162.74 | 176.42 |
| 736.6 | 148.06 | 154.98 | 168.19 |
| 787.4 | 139.35 | 146.75 | 159.95 |
| 838.2 | 131.61 | 140.06 | 149.40 |
| 889.0 | 121.93 | 131.20 | 138.19 |
| 939.8 | 112.05 | 119.30 | 126.60 |
| 990.6 | 101.74 | 108.39 | 114.37 |
| 1016 | 95.80 | 102.36 | 106.30 |

## 5 RESULTS

### 5.1 Residual Strength for Skin

The variation of the residual strength with the crack length for different values of skin thickness can represented in graphical form as shown in figure 5.1.

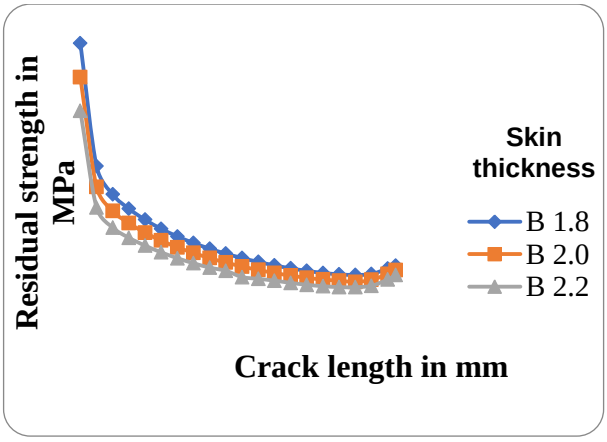


**Figure 5.1:** Residual strength graph for various skin thickness

### 5.2 Residual strength for bulkhead

The variation of the residual strength with the crack length for different values of skin thickness can represented in graphical form as shown in figure 5.2.

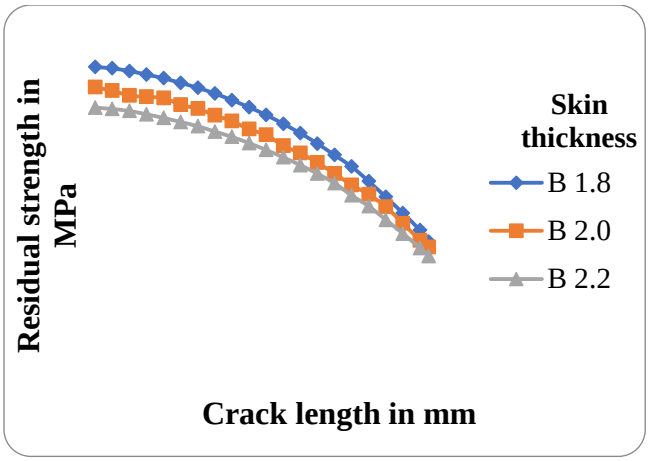


**Figure 5.2:** Residual strength of bulkheads for various skin thickness

## 6 DISCUSSIONS

The residual strength fluctuation of the bulkhead and skin of a stiffened panel with regard to crack propagation and skin thickness is shown in Figures 5.1 and 5.2. Figures 5.1 and 5.2 show that the residual strength of the skin and bulkhead decreases as the crack length increases. Due to the rise in skin thickness, the residual strength has also increased. For the same crack length and thickness, skin has the least residual strength of the two components. Because of the load transfer from the skin to the bulkheads, the residual strength of the skin is somewhat increased in that area.

## 7 CONCLUSION

The modified virtual crack closure integral approach used to assess the bulkhead's and skin's remaining strength in a stiffened panel produces reliable results. The methodology can therefore be used to assess the remaining strength of other parts of the stiffened panel.

**REFERENCES:**

[1] T. Swift, "Damage tolerance analysis of redundant structures," Fract. Mech. Des. Methodol. AGARD Lect. Ser. 97, p. 5, 1979.

[2] P. M. Toor, "A review of some damage tolerance design approaches for aircraft structures," Eng. Fract. Mech., vol. 5, no. 4, pp. 837–880, Dec. 1973, doi: 10.1016/0013-7944(73)90054-4.

[3] J. Wiggenraad, P. Arendsen, and J. da S. Pereira, "Design optimization of stiffened composite panels with buckling and damage tolerance constraints," in 39th AIAA/ASME/ASCE/AHS/ASC Structures, Structural Dynamics, and Materials Conference and Exhibit, American Institute of Aeronautics and Astronautics. doi: 10.2514/6.1998-1750.

[4] N. K. Salgado and M. H. Aliabadi, "An object oriented system for damage tolerance design of stiffened panels," Eng. Anal. Bound. Elem., vol. 23, no. 1, pp. 21–34, Jan. 1999, doi: 10.1016/S0955-7997(98)00058-7.

[5] M. Adeel, "Study on Damage Tolerance Behavior of Integrally Stiffened Panel and Conventional Stiffened Panel."

[6] S. Habeeb, "Crack arrest capabilities of an adhesively bonded skin and stiffener," Thesis, Wichita State University, 2012. Accessed: May 04, 2022. [Online]. Available: https://soar.wichita.edu/handle/10057/5596

[7] F. Carta and A. Pirondi, "Damage tolerance analysis of aircraft reinforced panels," Frat. Ed Integrità Strutt., vol. 5, no. 16, Art. no. 16, 2011, doi: 10.3221/IGF-ESIS.16.04.